Investigation of site-specific initiation and progress of alpha-synuclein pathology in Parkinson’s disease model

Nasrin Ahmed Tahrim
University of Helsinki
Faculty of Pharmacy
Division of Pharmacology
and Pharmacotherapy

May, 2025

HELSINGIN YLIOPISTO
HELSINGFORS UNIVERSITET
UNIVERSITY OF HELSINKI

Abstract

Faculty: Faculty of Pharmacy

Degree programme: Master's programme in pharmaceutical research, development and safety

Study track: Drug design and pharmacology

Author: Nasrin Ahmed Tahrim

Title: Investigation of site-specific initiation and progress of alpha-synuclein pathology in Parkinson's disease model

Level: Master's thesis

Month and year: May 2025

Number of pages: 31

Keywords: alpha-synuclein, Parkinson's disease, animal model, Lewy bodies, neurodegeneration, substantia nigra pars compacta, aggregates

Supervisor or supervisors: Aastha Singh, Merja H Voutilainen

Where deposited: University of Helsinki Library's digital archive HELDA

Abstract:

Parkinson's disease (PD) involves the gradual degeneration of dopamine-producing neurons in the substantia nigra pars compacta (SNpc) and the buildup of phosphorylated alpha-synuclein (pS129) inclusions—known as Lewy pathology, throughout the nervous system. Emerging data indicate that alpha-synuclein (aSyn) aggregates can propagate between neurons in a prion-like manner, yet the exact pathways and mechanisms by which this spread occurs are still not fully understood.

This thesis utilized a combined rat model involving unilateral injections of adeno-associated virus (AAV)-mediated human aSyn overexpression and pre-formed aSyn fibrils (PFF) to investigate the initiation and propagation of aSyn pathology. Rats were injected into four distinct sites (SNpc, amygdala, nose, gut) and evaluated at 6 and 12 months post-injection. Immunohistochemical staining assessed dopamine neuron integrity (TH-positive neurons), fiber density in the striatum, and distribution of pS129-positive aggregates across interconnected brain regions.

Injections into the brain (SNpc and amygdala) led to substantial aSyn aggregate formation and widespread propagation along anatomically connected pathways by 6 months, accompanied by significant dopamine neuron loss and striatal fiber degeneration specifically following SNpc injections. Peripheral injections (nose and gut) failed to induce detectable central pathology within the 12-month timeframe. Interestingly, despite progressive aSyn pathology, degeneration in the nigrostriatal pathway was reversed by 12 months, indicating stabilization or partial compensatory recovery.

These findings emphasize regional vulnerability and neural connectivity as crucial determinants of aSyn propagation and neurodegeneration. This combined AAV-aSyn+ PFF rat model effectively mirrors key aspects of PD progression, providing valuable insights into mechanisms underlying pathological spread and highlighting potential targets for therapeutic intervention.

HELSINGIN YLIOPISTO
HELSINGFORS UNIVERSITET
UNIVERSITY OF HELSINKI

Table of Contents

1 Introduction

Parkinson's disease (PD) ranks as the world's second most prevalent neurodegenerative condition, impacting approximately 7–10 million individuals globally (Duffy et al., 2018). While its hallmark motor features—slowness of movement (bradykinesia), resting tremor, muscle stiffness (rigidity), and balance problems, stem largely from degeneration of dopamine-producing neurons in the substantia nigra pars compacta (SNpc), PD is increasingly understood as a disorder affecting multiple systems. A range of non-motor issues such as reduced sense of smell (hyposmia), chronic constipation, disturbances in sleep patterns (including REM sleep behavior disorder), and alterations in mood or cognition—frequently emerge before, and persist alongside, the classic motor symptoms. Pathologically, PD is defined by two hallmarks: progressive neurodegeneration of midbrain nigrostriatal neurons and the accumulation of intraneuronal protein aggregates known as Lewy bodies (LBs) and Lewy neurites, collectively known as Lewy inclusions (Luk et al., 2012a). These Lewy inclusions consist of misfolded alpha-synuclein (aSyn) protein, as first demonstrated by Spillantini et al. in 1997 (Spillantini et al., 1997). aSyn is an abundant presynaptic protein of unclear normal function, but its aggregation into fibrillar, insoluble forms (often phosphorylated at serine-129) is a central feature of PD pathology. Indeed, while <5% of soluble aSyn is phosphorylated at S129 (pS129) under physiological conditions, ~90% of aSyn within Lewy bodies is phosphorylated at this residue, underscoring the close link between aSyn phosphorylation and toxic aggregation in PD (Fujiwara et al., 2002). The presence of aSyn inclusions (termed Lewy pathology) throughout the nervous system is a neuropathological signature of PD and related synucleinopathies, correlating not only with the classic motor deficits but also with the diverse non-motor symptoms that arise from extranigral involvement (Jellinger, 2011). PD's complex clinical picture – motor and non-motor – can be traced to the widespread distribution of aSyn pathology and associated neurodegeneration, making aSyn a focal point in understanding PD progression and developing disease models.

A growing body of evidence indicates that misfolded aSyn can propagate through the nervous system in a way that is prion-like, spreading pathology from cell to cell and region to region. Post-mortem staging studies by Braak and colleagues revealed that

Lewy body pathology in sporadic PD follows a remarkably stereotypical spatiotemporal pattern. In early stages (Braak Stage 1–2), aSyn aggregates are detected in the peripheral nervous system and lower brainstem – notably in the dorsal motor nucleus of the vagus (DMV) and the anterior olfactory structures – long before significant nigral degeneration occurs. As the disease advances, lesions appear in ascending fashion in the brainstem and midbrain (including the SNpc, Braak Stage 3), then spread to the limbic areas such as the amygdala and anteromedial temporal cortex (Stage 4), and finally to widespread neocortical regions in late stages (Stages 5–6). This progressive topography inspired the hypothesis that PD may begin in peripheral tissues (e.g. the gut or olfactory mucosa) and propagate upward to the brain – possibly triggered by an external pathogen or toxic insult that enters through the nasal and gastrointestinal routes. Such a "dual-hit" hypothesis (nasal and gastric entry) postulates that pathological aSyn might first emerge in the olfactory bulb and enteric nervous system, then invade the central nervous system via autonomic connections (Braak et al., 2003). Consistent with this idea, many early PD patients exhibit olfactory deficits and gastrointestinal dysfunction years before motor onset, reflecting likely aSyn pathology in the olfactory pathways and enteric vagal system (Calabresi et al., 2023).

The prion-like spread of aSyn provides a compelling explanation for PD progression. Misfolded aSyn can act as a "seed" that templates the misfolding of normal aSyn in connected cells, thereby self-propagating the lesion. In seminal studies, fetal dopamine neurons transplanted into the striatum of PD patients developed Lewy body inclusions a decade post-transplant, despite originating from a disease-free donor environment. This indicates that pathological aSyn species had transferred from the host PD brain into the healthy graft, in vivo – furnishing the first human evidence of the host-to-graft spread of Lewy pathology (Li et al., 2008). Parallel findings in animal models have reinforced the cell-to-cell transmission paradigm. For example, a single intrastriatal injection of synthetic aSyn fibrils into wild-type mice can induce PD-like neuropathology where the exogenous fibrils recruit endogenous aSyn to form pS129-positive Lewy body–like aggregates that progressively appear in anatomically interconnected regions, accompanied by the gradual loss of SNpc dopamine neurons and emergence of motor deficits (Luk et al., 2012b). This concept has profound relevance for modeling PD, as an

ideal model should replicate not just the endpoint lesions, but the progressive propagation of aSyn pathology over time.

Despite the centrality of aSyn in PD pathogenesis, conventional PD models have struggled to faithfully mirror the full spectrum of human PD pathology. Historically, toxin-based models (such as 6-hydroxydopamine lesions in rats, or systemic MPTP exposure in mice and primates) have been widely used. Toxin models produce acute degeneration of nigrostriatal dopamine neurons and robust motor impairments, and they have proven valuable for studying disease modifying treatments, dopamine cell death and testing symptomatic therapies. However, these models lack aSyn pathology, and the chronic progression seen in idiopathic PD. Although in the 1-methyl-4-phenyl-1,2,3,6-tetrahydropyridine/probenecid (MPTPp) chronic mouse model of PD there was a chronic tyrosine hydroxylase (TH)-positive cell degeneration (Schintu et al., 2009). Neurotoxin lesions typically do not exhibit Lewy bodies or pS129 aSyn aggregates, nor do they recapitulate the prodromal non-motor features or the spreading nature of the disease (Hassani & Esmaeili, 2024).

Transgenic models and viral vector models were the next step, incorporating aSyn itself into the modeling of disease. Multiple lines of transgenic mice (and some rats) overexpressing human aSyn (wild-type or PD-linked mutants like A53T) have been developed, as have models using adeno-associated viruses (AAV) to overexpress aSyn in targeted brain regions. These models often exhibit aSyn accumulation and can develop cellular changes or behavioral deficits related to PD. Nonetheless, transgenic/viral models also present important limitations. Overexpression at supraphysiological levels (often many-fold higher than normal aSyn expression) may drive non-physiological mechanisms of toxicity (Duffy et al., 2018b).

To better reproduce the progression and pathology of aSyn observed in PD, in this study we utilize a combined in vivo model that merges viral-driven aSyn overexpression with pre-formed fibril (PFF)-mediated seeding. Elevated aSyn levels would provide a vulnerable substrate, priming neurons to develop aggregates, while the introduction of misfolded aSyn seeds would jump-start the aggregation process – together precipitating

a more extensive and PD-like pathology than either alone (Thakur et al., 2017). This synergy suggests that a dual-hit approach – combining aSyn upregulation (to mimic genetic or age-related elevations of protein load) with pathological seeding (to mimic prion-like initiation) – can overcome the limitations of individual models and produce a pathology that better mirrors human PD. This study aims to evaluate how the spread of aSyn pathology and associated neurodegeneration evolves over time in a combined AAV-aSyn and pre-formed fibril (PFF) seeding rat model of Parkinson's disease. Specifically, we tried to address differences in pathology propagation from various injection sites to regions of the brain over time.

2 Materials and Methods

2.1 Animals

Adult Sprague–Dawley (SD) rats of both sexes (male and female), aged 5–8 months and weighing 250–300 g, were used for all experiments. Animals were group-housed under standardized temperature and humidity conditions on a 12-hour light/dark cycle, with unrestricted access to food and water. All procedures received approval from the National Animal Experiment Board of Finland and were conducted at the Laboratory Animal Center (LAC) core facility on the Viikki campus of the University of Helsinki, in compliance with institutional animal welfare guidelines.

2.2 Unilateral injections of AAV-aSyn +PFF

Each experimental rat received a unilateral injection of 5 µL solution containing equal parts AAV-aSyn and PFF. Specifically, 2.5 µL of an AAV vector encoding human aSyn was mixed with 2.5 µL of sonicated PFFs. The AAV-aSyn vector was obtained from the laboratory of Malin Parm (Lund University) and the PFFs were provided by Kelvin Luk (University of Pennsylvania) (Volpicelli-Daley et al., 2014). Injections were performed under general anesthesia and aseptic conditions. There were five experimental groups (2–3 rats each). In each group, the injection was targeted to one of four sites: the SNpc

(midbrain), the amygdala (forebrain), the nasal cavity (intranasal, targeting the olfactory pathways), or the gut (targeting the enteric nervous system). In all cases the injection was unilateral (administered to one side of the hemisphere) given in the right side of the brain while the left side was used as control. An additional control group of rats received no injection to serve as a baseline for comparisons. All injections were performed when the animals were between 3 and 4 months of age (this age was defined as post-injection, Day 0 of the experiment). Following the unilateral AAV-aSyn +PFF injection, the rats were returned to their home cages and monitored over long-term survival periods. Animals were sacrificed at 6 and 12 months post-injection to assess mid-term and long-term progression of pathology.

2.3 Immunohistochemistry

At the predetermined endpoints (6 or 12 months post-injection), animals were deeply anesthetized and perfused transcardially with 0.1 M phosphate-buffered saline (PBS) and then with 4% paraformaldehyde (PFA) in PBS. The brains were rapidly removed, post-fixed in 4% PFA for several hours (or overnight at 4 °C), and then cryoprotected in a buffered sucrose or antifreeze solution until they sank to prevent freezing artifacts. The brains were sectioned coronally at a thickness of 40 µm using a cryostat (LEICA CM 1950). Tissue sections were collected in a series such that every 7th section throughout the brain was retained for staining, providing a systematic random sampling of the rostral-to-caudal extent. All sections were kept free-floating and stored at –20 °C in an antifreeze cryoprotectant solution until further processing for immunohistochemistry. In order to to visualize tyrosine hydroxylase (TH, a dopamine neuron marker) and phosphorylated aSyn at serine-129 (pS129, a marker of pathogenic aSyn aggregates), as well as general neuronal architecture via Nissl staining, immunohistochemical staining was performed on free-floating brain sections. The brain regions of interest analyzed in this study included the SNpc, striatum, amygdala, hippocampus, DMV, and olfactory bulb. Unless otherwise stated, all incubations were done at room temperature (RT) and gentle agitation, and washes between steps were carried out in 0.1 M Tris-buffered saline (TBS).

2.4 TH and pS129 double staining in SNpc

Dual immunohistochemical staining for TH and pS129 was carried out on midbrain sections containing the SNpc to visualize the co-localization of dopamine neurons and aSyn aggregates. Sections were initially washed in TBS (three changes, 10 minutes each) before being treated with 0.3% H_2O_2 in TBS for 30 minutes to inactivate endogenous peroxidases. Following further washes, sections were blocked for one hour in TBS containing 1% BSA and 0.2% Triton X-100 to minimize non-specific antibody binding. They were then incubated overnight at 4 °C with a rabbit anti-pS129 aSyn primary antibody (1:1000; Abcam, Cat# ab51253) diluted in 0.5% BSA/TBS. After washing in TBS the next day, the tissues were exposed for one hour to a goat anti-rabbit biotinylated secondary antibody (1:400; Vector Laboratories, Cat# BA-1000). Sections were then incubated for one hour with an avidin–biotin–HRP complex (Vector Elite ABC kit, Vector Laboratories, Cat# PK-4004). Finally, pS129 immunoreactivity was revealed by developing the peroxidase reaction with nickel-enhanced DAB (Vector Laboratories, Cat# SK-4100). The sections were exposed to DAB substrate solution for approximately 2–3 minutes until a brown precipitate formed, indicating pS129-positive staining. The DAB reaction was stopped by transferring sections back to TBS, and sections were thoroughly rinsed to remove excess reagent.

To detect TH on the same sections, a second round of immunostaining was performed sequentially after the pS129 staining was completed. After the TBS washes, the tissue was incubated for 30 minutes in TBS containing 0.3% H_2O_2 to inactivate any residual peroxidase activity. In addition, an avidin/biotin blocking step was included at this stage: sections were treated sequentially with avidin and biotin blocking solutions (Vector Laboratories Avidin-Biotin Blocking Kit, Cat# SP-2001, 15 min each) to neutralize any free biotin or biotin-binding sites remaining from the previous ABC treatment. Following blocking, sections were incubated overnight at 4 °C with a mouse anti-TH primary antibody (1:2000; Millipore/Merck, Cat# MAB318) in TBS supplemented with 1% BSA and 0.05% Tween-20. The next day, after washing, sections were incubated for one hour to a goat anti-mouse biotinylated secondary antibody (1:400; Vector Laboratories, Cat# BA-9200), then incubated for an additional hour with the ABC peroxidase complex to

bind the biotinylated antibodies. TH immunoreactivity was visualized using HistoGreen (Linaris, Cat# E109) as the peroxidase substrate, which produces a green reaction product. The HistoGreen solution was applied for about 2 minutes, or until a green coloration of TH-positive cells and fibers were evident, and then sections were rinsed in distilled water to stop the reaction. Through this sequential double-staining procedure, TH-positive dopamine neurons (green labeling) and pS129-positive aSyn inclusion bodies known as phosphorylated aSyn, paSyn (brown labeling) could be identified in the same SNpc tissue sections. After completing the staining, sections were mounted onto glass slides, allowed to air-dry, and later dehydrated and cover slipped as described below.

2.5 TH-DAB staining in striatum

To evaluate dopamine nerve fiber innervation in the striatum, an immunohistochemical staining for TH was performed on a separate series of striatal sections, using a single-label DAB protocol. Free-floating striatal sections were processed essentially as described above for TH in the SNpc, except without a preceding pS129 staining step. In brief, sections were rinsed and treated with 0.3% H_2O_2 in TBS for 30 min to block endogenous peroxidase, followed by a 1-hour block in 1% BSA/0.2% Triton X-100. Sections were then incubated overnight at 4 °C with the mouse anti-TH primary antibody (1:2000, Millipore MAB318) in 0.5% BSA/TBS. After TBS washes, a biotinylated goat anti-mouse secondary antibody (1:400, Vector BA-9200) was applied for 1 hour at RT. The signal was amplified with the ABC method for 1 hour and visualized with DAB as the chromogen (developing a brown reaction product for ~2 minute or until it became distinctly stained). Stained sections were rinsed, mounted on slides, and dried. The resulting DAB labeling of TH-positive fibers in the striatum was used for subsequent quantification of dopamine fiber density.

2.6 pS129 and Nissl Staining

In order to examine the spread and distribution of aSyn pathology in various brain areas, additional sections from the striatum, amygdala, hippocampus, olfactory bulb, and DMV

were processed for pS129 immunohistochemistry and Nissl counterstaining. Free-floating sections from these regions were first immunostained for pS129 as described above (using the rabbit anti-pS129 primary antibody at 1:1000 and DAB for visualization). This single label pS129 staining was performed on sections representing each region of interest. After developing the pS129 stain with DAB (yielding brown labeled inclusions), the sections were rinsed and subsequently counterstained with 0.1% Cresyl Violet acetate (Nissl stain) for approximately 5–10 minutes. The Cresyl Violet stained Nissl substance in neuronal cell bodies a purple-blue color, providing anatomic context and allowing visualization of the overall neuronal architecture in the section. Following Nissl staining, sections were dehydrated through a graded ethanol series (50%, 70%, 95%, 100% ethanol), cleared in xylene, and mounted with DPX mounting medium under coverslips. This counterstaining procedure enabled the identification of brain region landmarks and the assessment of pS129-positive inclusion location relative to the total neuronal population in each region.

(Note: After completion of any of the above staining protocols, tissue sections were typically mounted onto gelatin-coated microscope slides, air-dried overnight, and then passed through ascending ethanol concentrations and xylene before being coverslipped with DPX or similar permanent mounting media. This ensured long-term preservation of the tissue and allowed for high-quality imaging).

2.7 Quantification and imaging

For quantitative analysis, all immunostained slides were scanned to create high-resolution digital images. Whole-slide imaging was performed at 20× magnification with extended depth of field using a 3DHISTECH Pannoramic P250 slide scanner (3DHISTECH Ltd., Budapest, Hungary). The resulting digital images were visualized and analyzed with the 3DHISTECH SlideViewer software. To assess dopamine cell loss, the number of TH-positive neurons in the SNpc was counted manually on the scanned images. Likewise, the number of pS129-positive intracellular aggregates (Lewy body-like inclusions) in each region or section was manually quantified. These counts were performed in a blinded fashion for all animals, focusing on the injected hemisphere of the brain. Densitometric

measurement of TH-positive fiber innervation in the striatum was carried out using ImageJ software (National Institutes of Health, USA). For each animal, equivalent striatal sections (at a consistent rostrocaudal level) were chosen, and the optical density of the DAB-labeled TH staining in the striatum was measured as an index of dopamine fiber density. Background staining was subtracted using adjacent unlabeled areas to obtain a specific TH signal density. For presentation of histological data, representative photomicrographs of stained sections were exported from SlideViewer and arranged into figure panels using Microsoft PowerPoint. Care was taken to select brain sections at comparable anatomical levels across all experimental groups when making comparisons, ensuring that images and counts reflected the same region and coordinate in each animal.

2.8 Statistical analysis

Statistical analyses were conducted in GraphPad Prism (v. 10.4.1; GraphPad Software, San Diego, CA). Data are reported as mean ± SEM unless specified otherwise. Group differences were assessed by one-way ANOVA. If ANOVA revealed a significant effect, post hoc tests were performed: Sidak's test for specific pairwise comparisons or Dunnett's test for comparing each treatment group to the control. A two-tailed p-value below 0.05 was considered statistically significant, and equal variances were assumed unless homogeneity tests suggested otherwise.

3 Results

This study examined the effects of combined AAV-aSyn and PFF injections in rats. Five experimental groups received unilateral injections into one of four sites: the SNpc, amygdala, nasal cavity (olfactory route), or gut; a fifth group served as uninjected control. The focus was on assessing neurodegeneration and the propagation of aSyn pathology in key brain regions: the SNpc, striatum, amygdala, hippocampus, DMV, and olfactory bulb. Animals were sacrificed at 6 or 12 months post-injection for analysis. Neurodegeneration was evaluated by quantifying TH-postive cell bodies in the SNpc and TH-positive fiber density in the striatum, while the spread of pathological aSyn was tracked by immunohistochemical detection of pS129 aggregates. All injections were made

unilaterally into the right hemisphere, with the left hemisphere serving as an internal control (i.e., contralateral side with no treatment).

3.1 Propagation of aSyn pathology

Figures 1 and 2 show representative immunostaining for pS129 aSyn aggregates (brown) alongside TH labeling (green) in six brain regions at 6 months (Figure 1) and 12 months (Figure 2) after AAV-aSyn+ PFF delivery. At 6 months post-injection (Figure 1), pronounced aSyn pathology was observed only in animals that received injections into the brain (SNpc or amygdala), whereas peripheral (nose or gut) injections did not produce any detectable aggregates in any brain region. In SNpc-injected rats, pS129 aggregates had propagated to several connected regions. The ipsilateral striatum showed scattered brown aSyn deposits (Figure 1c), and inclusions were evident in limbic areas such as the amygdala and hippocampus (Figure 1d, e). In contrast, the injected SNpc itself (Figure 1 f, right side) contained very few visible inclusions at this stage, even though TH-positive neuron staining was markedly reduced there (indicating neuron loss, see Section 3.2). Moreover, the TH-positive fibers in striatum showed a marked reduction in fiber density compared to control side (Figure 1 b). Notably, regions lacking direct neural connections to the SNpc—such as the olfactory bulb and the DMV—showed no pS129 pathology (Figure 1a, g). Amygdala-injected rats exhibited a different pattern consistent with limbic network spread: by 6 months a dense accumulation of aSyn aggregates was present within the ipsilateral amygdala (Figure 1d), with some spread to the striatum (Figure 1c). A few inclusions appeared in the connected entorhinal cortex, but other regions (including the SNpc, olfactory bulb, and DMV) remained essentially free of pathology. As expected from the lack of SNpc involvement, amygdala-injected animals also did not show any loss of SNpc TH-positive neurons at this time (Figure 1a, amygdala column, showing intact TH staining in SNpc). In contrast, nasal and gut injections did not induce detectable pS129 aggregates in any brain region at six months. Neither the olfactory bulb, hippocampus nor the brainstem (including DMV) of these peripheral-injection animals contained aggregates, indicating little or no central uptake or transport of misfolded aSyn from the nose or gut within the first six months.

Taken together, the 6 months data demonstrate an early and site-specific propagation of pathological aSyn from central injection sites (SNpc or amygdala) but not from peripheral sites (nose or gut). Furthermore, only anatomically connected regions developed aggregates, whereas disconnected areas (for example, the olfactory bulb for SNpc injections, or the SNpc for amygdala injections) showed no pathology.

By 12 months post-injection, the burden of aSyn inclusions had increased markedly in the central injection groups, while remaining absent in the peripheral groups (Figure 2). In SNpc-injected rats, pS129 aggregates became far more abundant and widespread by one year. The previously modest pathology in the SNpc itself had grown into dense, dark-brown intracellular inclusions throughout the ipsilateral SNpc (Figure 2f), and the striatum—an axonal projection target of SNpc neurons—contained a profusion of aggregates (Figure 2c), although, the TH-positive fiber in the striatum was not affected (Figure 2b). The propagation of aSyn pathology into limbic circuits was also more pronounced: numerous aggregates were present in the amygdala and (Figure 2d, e), far more than seen at 6 months. Despite this extensive spread, the olfactory bulb and DMV (Figure 2a, g) still exhibited no detectable pathology in SNpc-injected rats, indicating that aSyn spread continued to follow established neuronal pathways rather than diffusing non-specifically to remote regions. Amygdala-injected rats at 12 months displayed extensive limbic pathology localized to connected regions. The amygdala itself had densely packed pS129 inclusions (even more than at 6 months), and its neighboring or synaptically connected areas—such as the hippocampus and striatum—acquired additional aggregates (Figure 2b–e). Yet, midbrain regions (e.g., the SNpc) and distal areas like the olfactory bulb and DMV remained largely unaffected in the amygdala injection group, suggesting that the spread was confined to the limbic network initiating from the amygdala. Meanwhile, nose and gut injected animals continued to show no central aSyn pathology even after one year; critical regions such as the olfactory bulb (the primary target for nasal entry) or the DMV (initial entry for gut-vagal routes) were completely devoid of pS129 staining. This confirms that peripheral seeding was insufficient to trigger any noticeable brain aSyn pathology within the studied timeframe.

In summary, the spreading pattern of pS129 immunostaining at 6 and 12 months indicates that aSyn aggregates propagate outward from the site of a central injection along neural connections. SNpc seeding led to progressive involvement of the connected nigrostriatal and mesolimbic pathways, whereas amygdala seeding resulted in pathology confined to limbic circuits. The control group exhibited no detectable aSyn pathology or dopaminergic neurodegeneration at either the 6 or 12 months timepoint. Crucially, neither paradigm showed invasion of regions lacking direct connectivity (such as the olfactory bulb or vagal nuclei), and no pathology emerged from peripheral-only challenges. These findings highlight a network-specific spread of aSyn pathology originating from central nervous system injection sites.

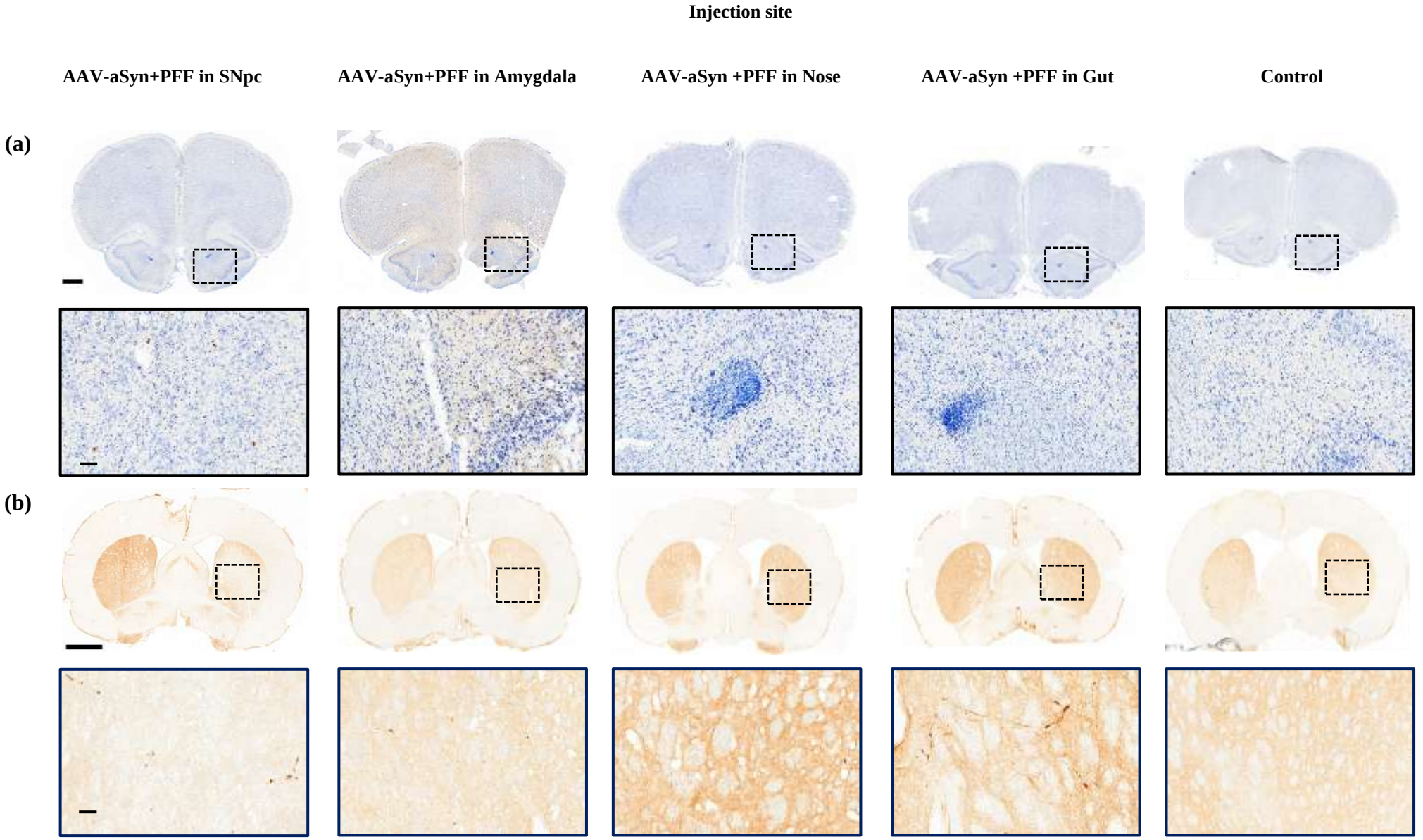
Injection site
AAV-aSyn+PFF in SNpc
AAV-aSyn+PFF in Amygdala
AAV-aSyn +PFF in Nose
AAV-aSyn +PFF in Gut
Control
(a)
(b)

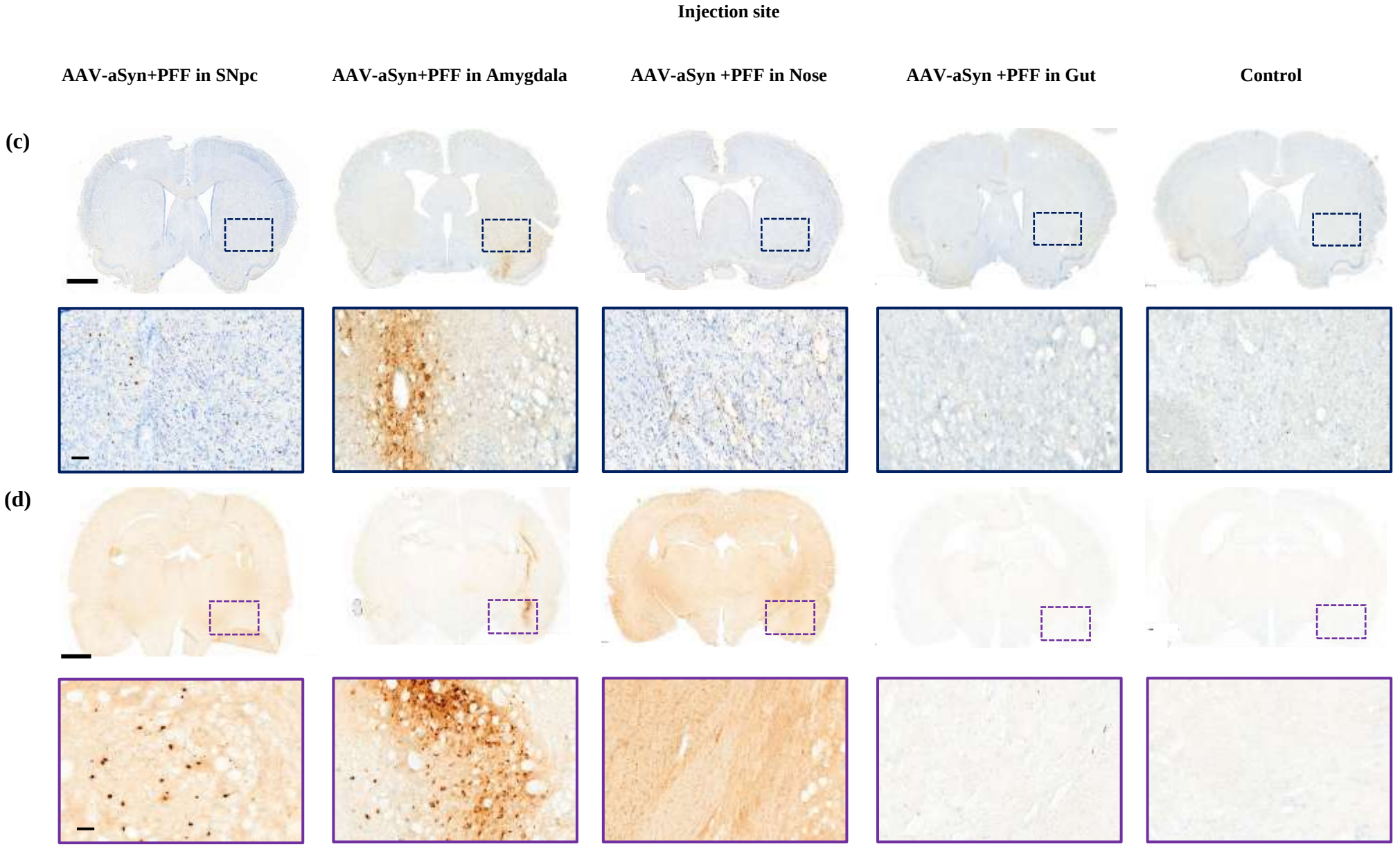
Injection site
AAV-aSyn+PFF in SNpc
AAV-aSyn+PFF in Amygdala
AAV-aSyn +PFF in Nose
AAV-aSyn +PFF in Gut
Control
(c)
(d)

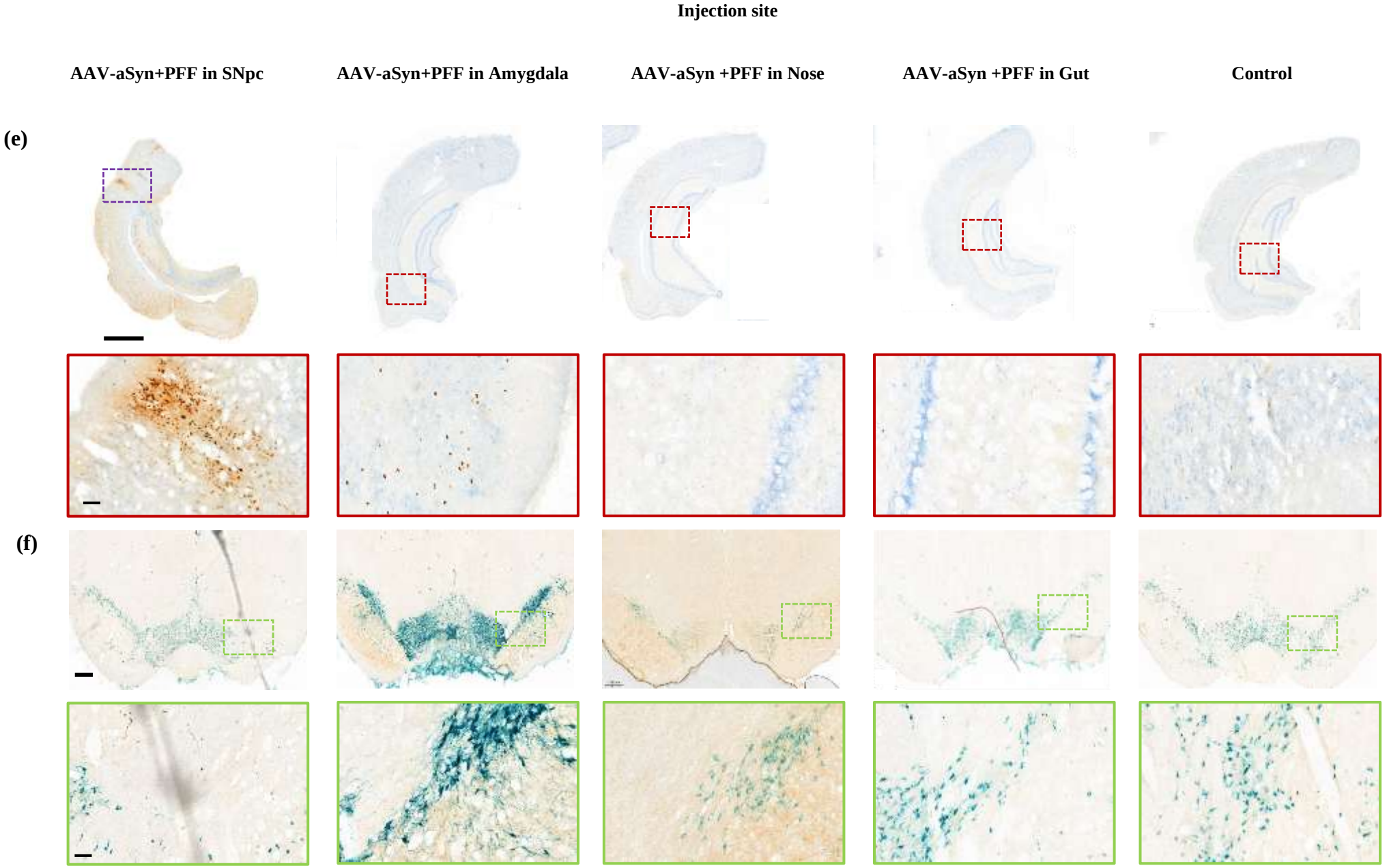
Injection site
AAV-aSyn+PFF in SNpc
AAV-aSyn+PFF in Amygdala
AAV-aSyn +PFF in Nose
AAV-aSyn +PFF in Gut
Control
(e)
(f)

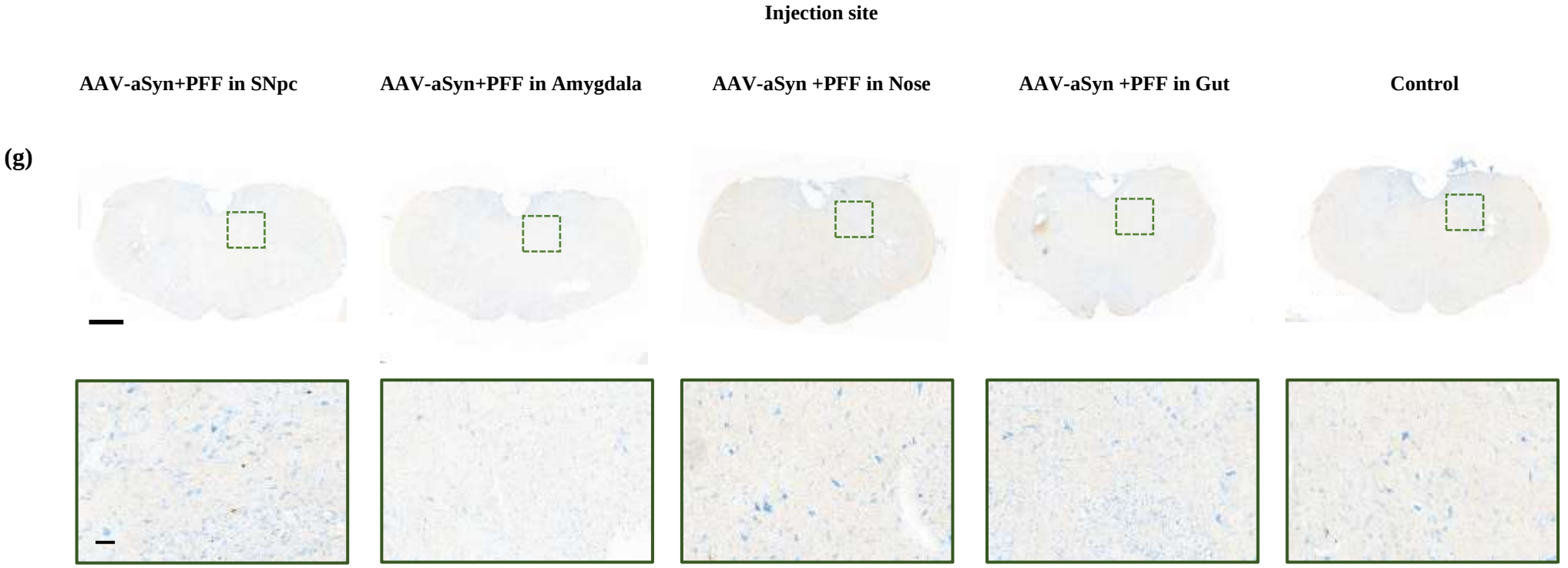

Figure 1: aSyn pathology and TH-positive neuron survival at 6 months post-injection. Representative immunohistochemical images from a rat injected with AAV-aSyn + PFF into the right side of the brain and into the nose and gut, TH-positive dopamine neurons/fibers (are visible in green), pS129 aggregates, in brown, and cell nuclei, NISSL in blue. Six brain regions are displayed, each with a low-magnification overview and a higher-magnification inset to highlight cellular detail. (a) Olfactory bulb (b) Striatum- TH-labeled-DAB (c) Striatum-pS129 and NISSL (d) Amygdala (e) Hippocampus; magnified at low 1x and high 10x magnification (scale bars are 2mm and 0.100mm) (f) SNpc – at low 2× and high 10× magnification (scale bars are 0.500mm and 0.100mm). (g) DMV; magnified at low 1x and high 10x magnification (scale bars are 2mm and 0.100mm)

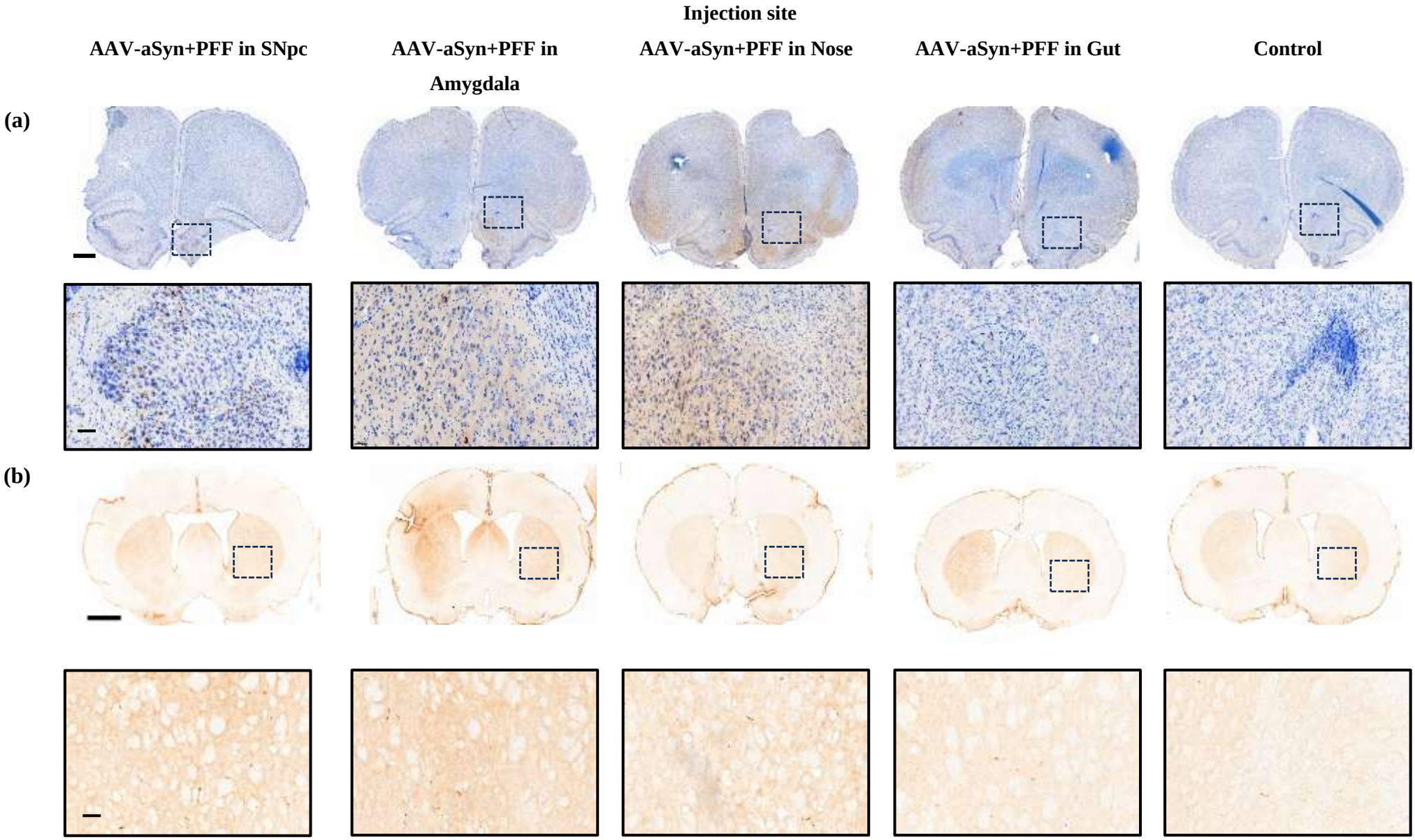
Injection site
AAV-aSyn+PFF in SNpc
AAV-aSyn+PFF in Amygdala
AAV-aSyn+PFF in Nose
AAV-aSyn+PFF in Gut
Control
(a)
(b)

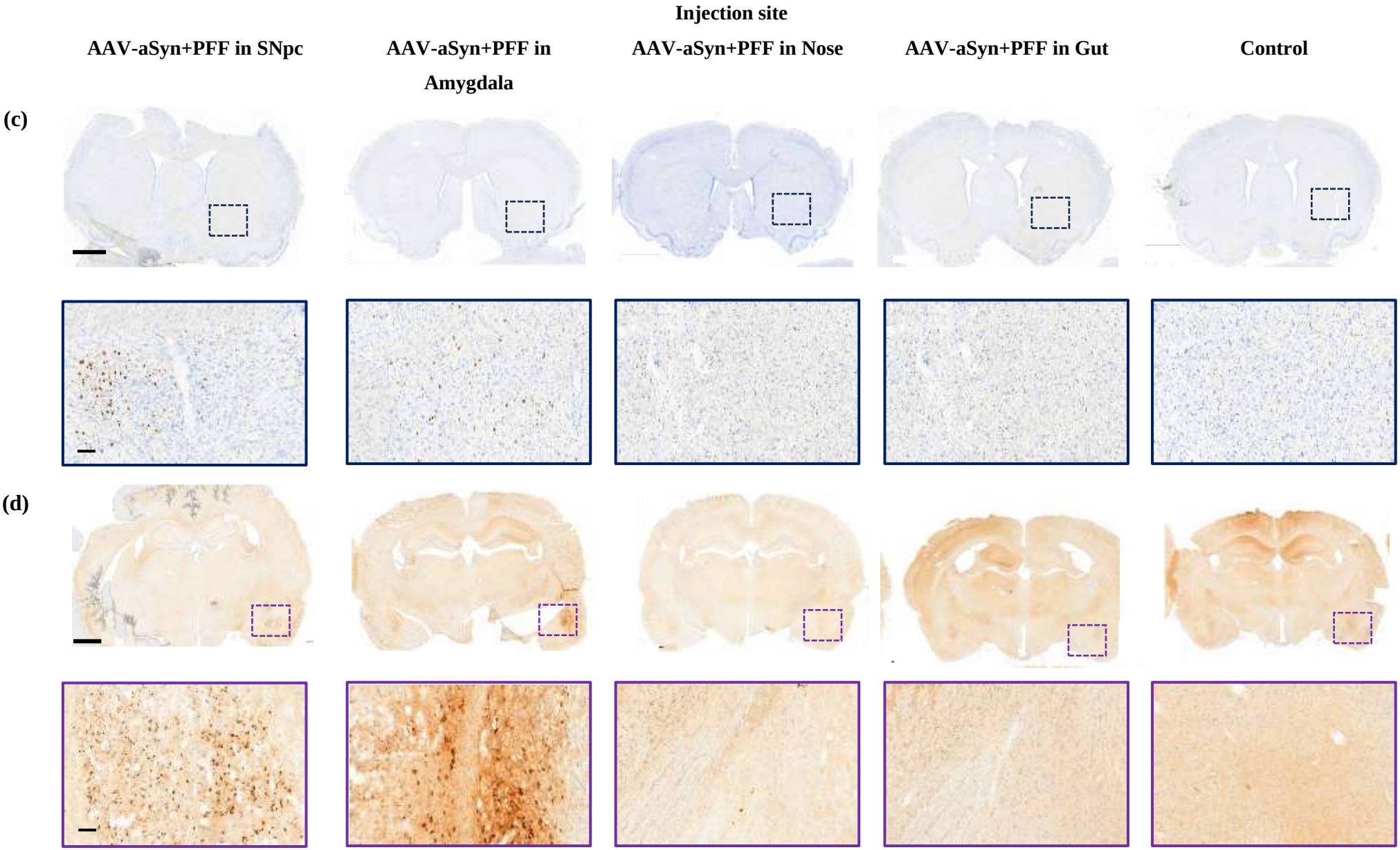
Injection site
AAV-aSyn+PFF in SNpc
AAV-aSyn+PFF in Amygdala
AAV-aSyn+PFF in Nose
AAV-aSyn+PFF in Gut
Control
(c)
(d)

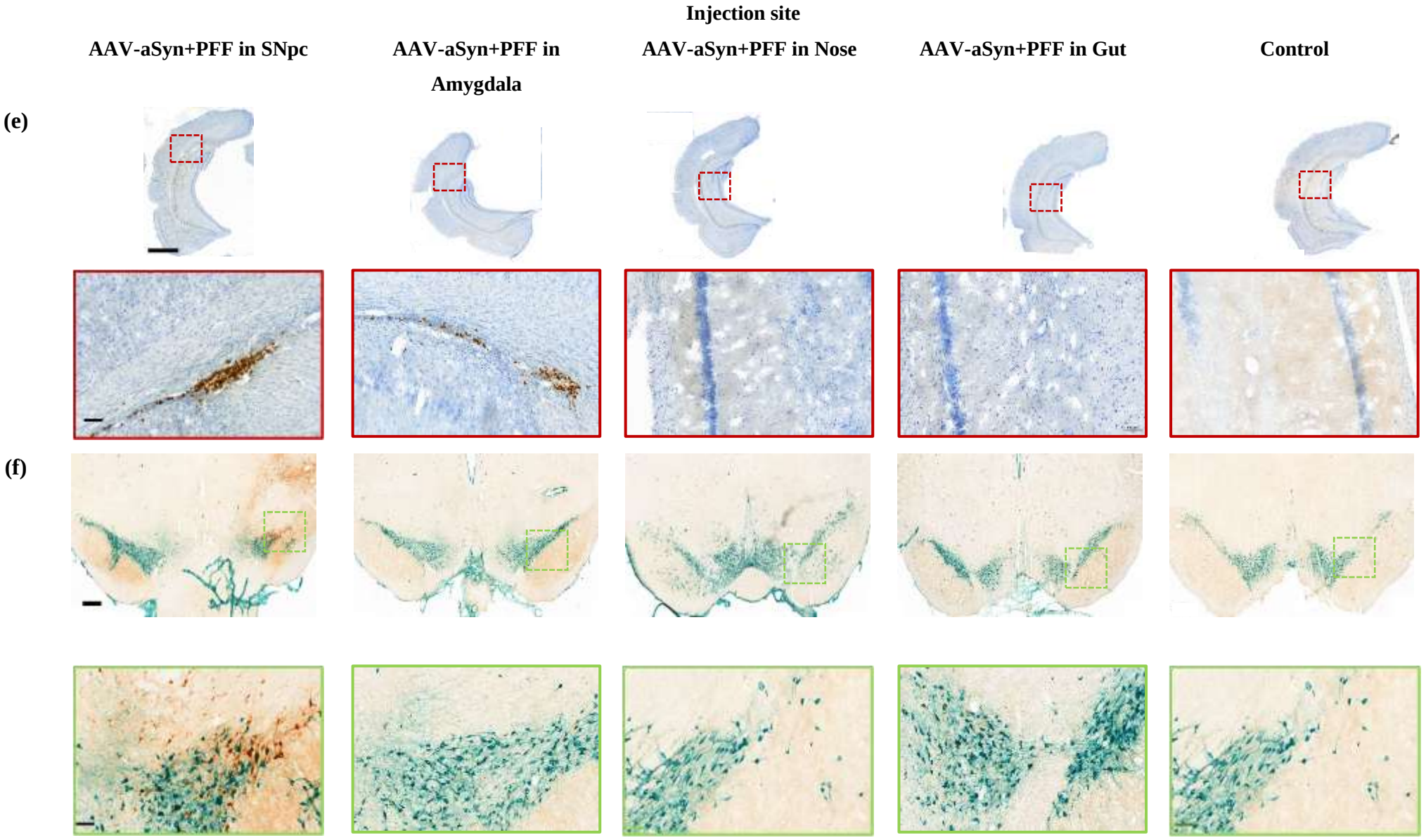
Injection site
AAV-aSyn+PFF in SNpc
AAV-aSyn+PFF in Amygdala
AAV-aSyn+PFF in Nose
AAV-aSyn+PFF in Gut
Control
(e)
(f)

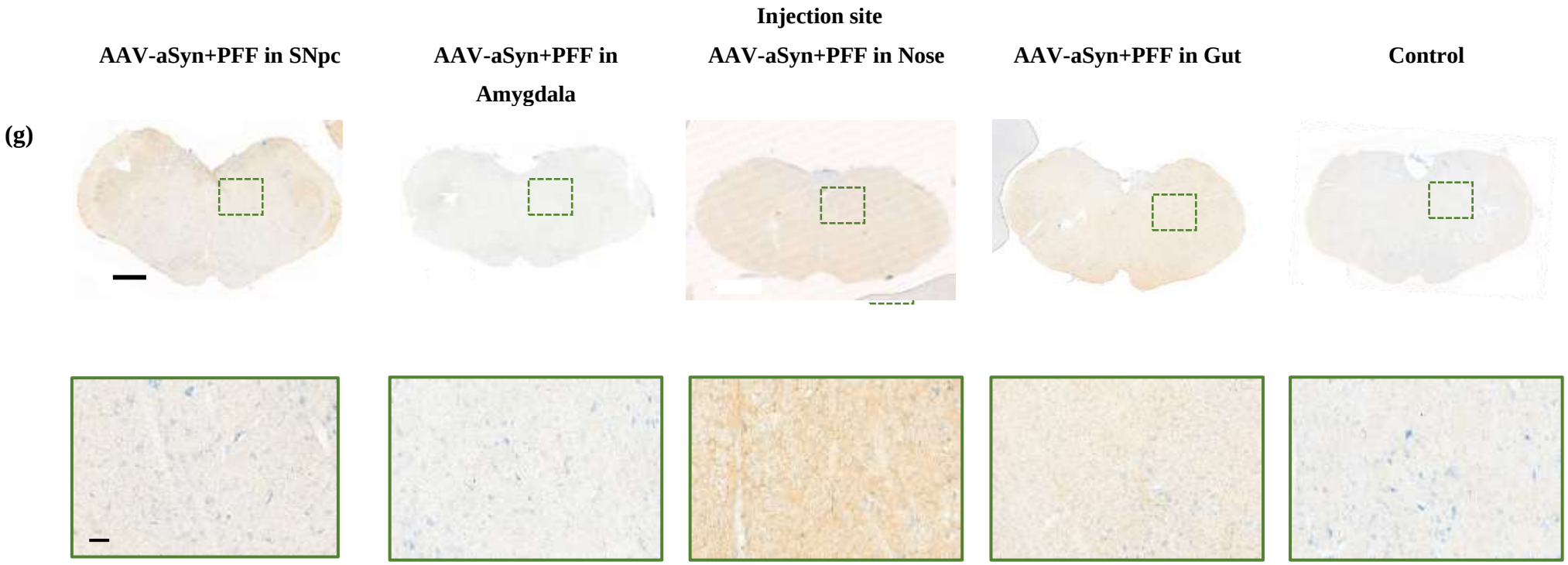

Figure 2: aSyn pathology and TH-positive neuron survival at 12 months post-injection. Representative immunohistochemical images from a rat injected with AAV-aSyn + PFF into the right side of the brain and into the nose and gut, TH-positive dopamine neurons/fibers (are visible in green), pS129 aggregates, in brown, and cell nuclei, NISSL in blue. Six brain regions are displayed, each with a low-magnification overview and a higher-magnification inset to highlight cellular detail. (a) Olfactory bulb (b) Striatum- TH-labeled-DAB (c) Striatum-pS129 and NISSL (d) Amygdala (e) Hippocampus; magnified at low 1x and high 10x magnification (scale bars are 2mm and 0.100mm) (f) SNpc – at low 2× and high 10× magnification (scale bars are 0.500mm and 0.100mm). (g) DMV; magnified at low 1x and high 10x magnification (scale bars are 2mm and 0.100mm)

3.2 TH-positive Cell Loss in SNpc

To assess dopaminergic neuron degeneration, TH-positive cells in the SNpc were counted in the injected (ipsilateral) versus non-injected (contralateral) hemispheres at 6 and 12 months. At 6 months, although not statistically significant, a loss of SNpc dopamine neurons was detected, but only in the group that received an SNpc injection. These rats had approximately 56.5 ± 21.2% TH-positive neurons in the ipsilateral SNpc, compared to 114.2 ± 21.2 % TH-positive neurons in the contralateral side – roughly a 50% reduction in neuron count. This difference is illustrated by the diminished TH staining in the right SNpc of SNpc-injected animals (Figure 1f, SNpc column) and is quantified in Figure 3a. One-way ANOVA confirmed a significant treatment effect on SNpc cell counts ($F(4,21) = 3.656$, $p = 0.0207$, $R^2 = 0.41$), and Šídák post-hoc analysis indicated that the SNpc-injected group had significantly fewer SNpc neurons than controls (adjusted $p = 0.0505$, narrowly meeting the significance criterion). No other injection group exhibited notable cell loss in the SNpc at 6 months: rats injected in the amygdala, nose, or gut all retained TH-positive cell counts in the ipsilateral SNpc that were statistically indistinguishable from controls. By 12 months, the apparent TH-positive cell loss in SNpc-injected rats had recovered, and differences between groups had largely evened out (Figure 3b). SNpc-injected animals still showed reduced TH neuron counts relative to their contralateral side, but this reduction was not significant and instead it decreased from 50% TH-positive cell loss to only 20%. Moreover, around 10% or less loss of TH-positive neurons was also observed in control and non-SNpc groups by 12 months (potentially due to aging or variability), such that the overall group effect was no longer significant. A one-way ANOVA at 12 months found no reliable differences in TH-positive cell counts among the five groups ($F(4,9) = 1.429$, $p = 0.3008$). Thus, by one year post-injection, there was no statistical distinction in SNpc TH-positive neuron between the groups.

3.3 Striatal Fiber Degeneration

We next examined degeneration of dopamine nerve terminals in the striatum by measuring TH-positive fiber density in the dorsal striatum of each hemisphere. At 6 months post-injection, TH-positive fibers in the striatum exhibited significant degeneration in the SNpc-injected group, mirroring the SNpc cell body loss. In the contralateral (control) striatum of SNpc-injected rats, TH fiber density averaged 108.4 ± 13.7%, whereas the ipsilateral striatum had only 60.2 ± 13.7%, corresponding to an approximately 44% loss of dopamine fibers. This loss

of striatal innervation is evident in Figure 1f (SNpc injection column), which shows visibly reduced green TH fiber staining on the injected side, and is quantified in Figure 3c. A one-way ANOVA revealed a significant group effect on striatal TH fiber density ($F(4,7) = 4.363$, $p = 0.0439$, $R^2 = 0.71$). Post-hoc comparison using Dunnett's test confirmed that only the SNpc-injected group had a significantly lower striatal fiber density compared to the control (no-injection) group ($p = 0.0284$). In contrast, rats injected in the amygdala, nose, or gut showed no significant loss of striatal TH fibers at 6 months, consistent with their intact SNpc cell counts. Figure 3c illustrates that the mean striatal fiber densities for these other groups remained near 100% of contralateral levels, whereas the SNpc group was markedly lower. By 12 months, there was no further progression of striatal fiber loss in the SNpc-injected animals, and no new deficits emerged in any other group (Figure 3d). Quantitatively, TH innervation in the SNpc-injected striatum remained at lower level (approximately at 80%) compared to the 60% observed at 6 months, and the overall one-way ANOVA for striatal fiber density was not significant at 12 months ($F(4,9) = 0.424$, $p = 0.7881$). Thus, similar to the SNpc cell body counts, striatal TH fiber density reached a stable low point by 6 months in the SNpc-seeded group and then recovered at 12 months. No differences were detected between groups at the one year time point, indicating that only the early SNpc seeding had a measurable impact on striatal dopamine innervation, with no late-onset degeneration in the other conditions.

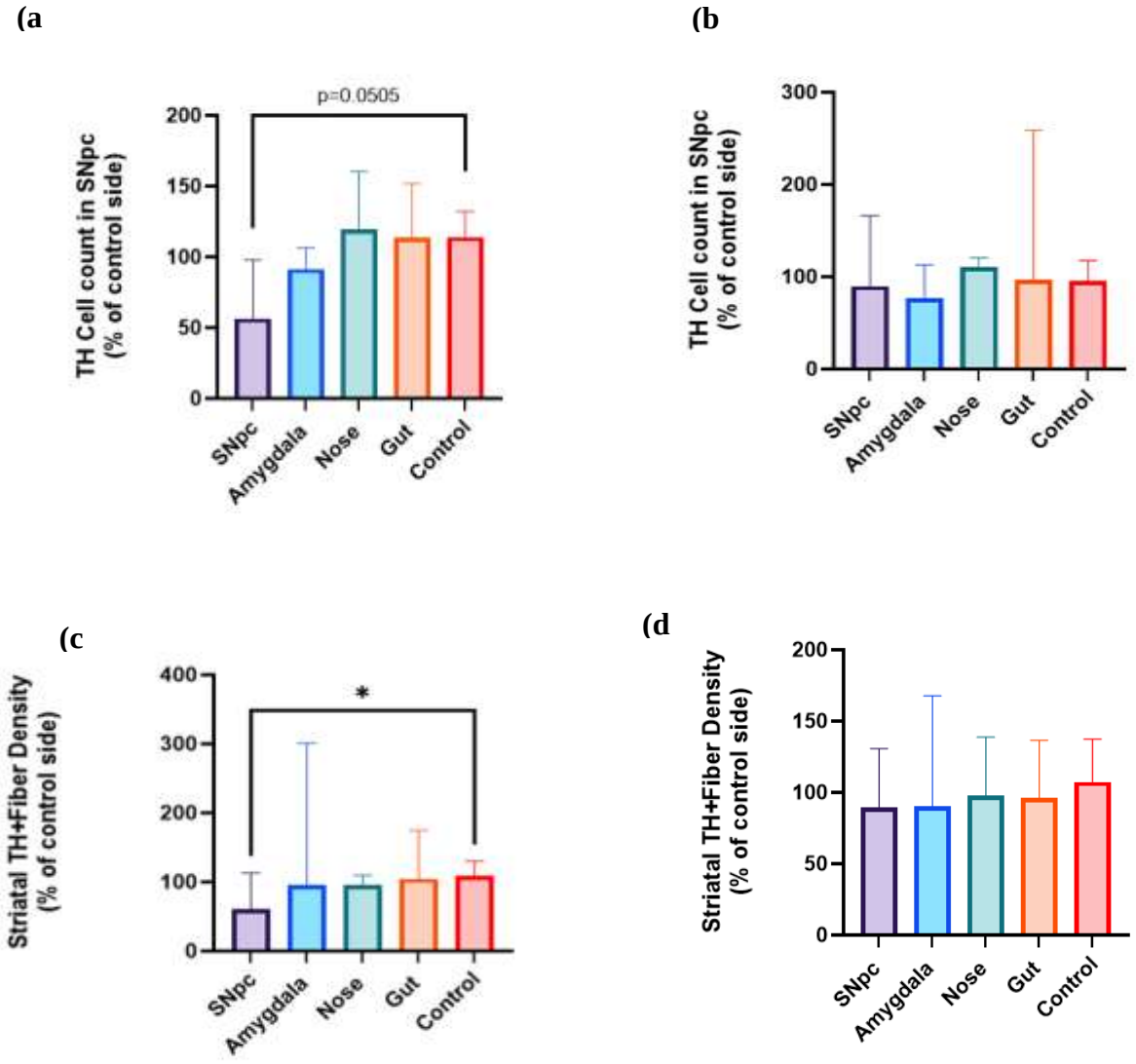

Figure 3: TH-positive neuron and fiber quantification at 6 and 12 months. Bar graphs show mean TH-positive cell counts in the SNpc after (a) 6 and (b) 12 months and TH-positive fiber density in the striatum after (c) 6 and (d) 12 months as percentages of the contralateral control side, with error bars indicating 95% confidence intervals. Statistical comparisons were performed using one-way ANOVA with Šídák or Dunnett's post-hoc tests, n=2-3 animals per group, *p<0.05.

3.4 Dopamine Nigrostriatal Pathway

Assessment of TH immunoreactivity provided insight into the integrity of the dopamine nigrostriatal pathway. At 6 months post-injection, animals injected directly into the SNpc displayed substantial degeneration, evident as a pronounced reduction in TH-positive neurons within the SNpc (Figure 1f) and a corresponding loss of TH-positive nerve fibers within the ipsilateral striatum (Figure 1b). Quantitatively, SNpc-injected animals showed approximately a 50% decrease in TH-positive neuron counts compared to the contralateral, non-injected

hemisphere (Figure 3a). This neuronal loss was matched by a parallel reduction in striatal TH-positive fiber density, which was significantly reduced to roughly 60% of the contralateral side (Figure 3c; ANOVA, $F(4,7) = 4.363$, $p = 0.0439$). Post-hoc Dunnett's analysis confirmed a statistically significant reduction specifically in the SNpc-injected group ($p = 0.0284$ vs. controls).

This strong correlation between neuron loss in the SNpc and fiber degeneration in the striatum aligns closely with the known anatomical trajectory of dopamine axons projecting from the SNpc to the striatum. Damage to dopamine cell bodies thus directly leads to the degeneration of their connected nerve terminals, a phenomenon consistently observed in various models of PD and other neurodegenerative conditions involving long-projecting neuronal populations (Cheng et al., 2010).

By 12 months post-injection, both SNpc neuron numbers and striatal fiber densities had stabilized, showing no further significant decline relative to the levels observed at 6 months. At this later timepoint, neuron counts remained at approximately 80% of contralateral control levels, and striatal fiber density similarly stabilized around 80%, indicating partial structural recovery or halted degeneration (Figure 3b, d). ANOVA confirmed that the differences were not significant among groups at 12 months, indicating that the degenerative process plateaued, with surviving neurons potentially undergoing compensatory mechanisms to preserve dopamine function.

Together, these results emphasize the vulnerability of dopamine neurons in nigral and their projecting fibers to aSyn pathology, confirming the essential role of the SNpc-striatum connection in disease progression and recovery dynamics within the nigrostriatal dopamine system.

4 Discussion

PD is a multifaceted neurodegenerative disorder involving interacting environmental, genetic, and cellular factors that lead to motor and non-motor symptoms (Poewe et al., 2017). However, no existing model incorporates all these factors, which hinders the progress in developing therapies that modify the course of the disease. This study presents a model of PD pathology using a combined AAV-aSyn overexpression and PFF seeding approach in rats. Overall, our

findings provide evidence for prion-like aSyn aggregate propagation and associated neurodegeneration in a region-specific manner. By 6 months post-injection, we observed substantial dopamine cell loss in the SNpc-injected rats accompanied by pS129 aggregate accumulation in the SNpc and its projection area, the striatum. Notably, by 12 months the pathology had further propagated to additional interconnected regions (including parts of the limbic system such as the amygdala and hippocampus), yet no aggregates were visible in regions like the DMV and the olfactory bulb. Similarly, by 12 months post-injection, the remaining SNpc neurons exhibited elevated TH expression and the density of TH-positive fibers in the striatum had plateaued, suggesting a degree of structural recovery in the dopamine system.

4.1 Prion-like propagation and region-specific pathological pattern of pS129 aggregate

Our observations strongly support the concept that misfolded aSyn can self-propagate and spread through neural circuits in a manner that is prion-like. The spread of aSyn from site of injection to other regions of the brain connected by synapses supports the idea of cell to cell transmission of pathogenic aSyn. This finding is consistent with previous study by Luk et al. (2012), who showed that a single intrastriatal injection of aSyn PFFs in wild-type mice led to the templated misfolding of endogenous aSyn and the appearance of LB-like inclusions in anatomically connected areas (Luk et al., 2012). In Luk's study, the gradual accumulation of LBs that eventually caused degeneration of dopamine neurons in SNpc, while leaving neighboring areas like the ventral tegmental area (VTA) unaffected, as consistent with our study. Similarly, Recasens et al., (2014) demonstrated with an alternative paradigm – injecting brain-derived LB extracts – that human pathological aSyn can seed host aSyn and induce PD-like changes in recipient animals. These studies, consistent with our results, support the idea that introduction of misfolded aSyn trigger the spread of pathological aggregates through interconnected neuronal pathways, initiating a progressive neurodegenerative process (Recasens et al., 2014).

Crucially, our model combines aSyn overexpression with PFF seeding, and this was expected to amplify the prion-like spreading effect. Previous studies had suggested that providing an excess of aSyn in host neurons would intensify seeding outcomes and accelerate pathology. For example, Luk et al. found that PFF injections in non-overexpressing mice required several months to induce widespread inclusions and cell loss. In contrast, Thakur et al. (2017) reported

that elevating aSyn levels via AAV greatly accelerates and intensifies PFF-induced pathology: with combined AAV+PFF, Lewy-like inclusions were observed within days of the fibril injection, accompanied by rapid dopamine neuron degeneration (Thakur et al., 2017). This synergistic effect likely arises because overexpressed aSyn provides an abundant substrate for templated conversion, making neurons more susceptible to seeding. Consistent with that idea, mice lacking endogenous aSyn are completely resistant to PFF-induced propagation (no CNS pathology occurs without host aSyn (Chen et al., 2023). Our results at 6–12 months post-injection extend these concepts to a longer timeframe, showing that the presence of misfolded aSyn seeds in the rat brain can initiate a self-perpetuating pathology that expands gradually. The aggregate spread we observed – from the SNpc to the striatum and further to connected regions like the amygdala and hippocampus by one year – underscores the slow but relentless nature of prion-like propagation in vivo (comparable to the staging in Luk et al., 2012b).

Although aSyn aggregates have a wide ability to spread, our data also emphasize that specific brain regions did not have any aggregates, suggesting region-specific variations in vulnerability or connectivity. In particular, we found that the DMV in the medulla and olfactory bulb showed no detectable aSyn pathology even at 12 months. This is in contrast with the Braak staging hypothesis of idiopathic PD, which states that PD pathology often begins in the peripheral nervous system (such as the enteric nervous system and DMV) or olfactory structures and then ascends to the midbrain (Braak et al., 2003; Visanji et al., 2014). In our model, the opposite sequence was present: pathology was initiated in the midbrain and spread outward, while the far-caudal brainstem and olfactory regions (which would be early sites in Braak's hypotheses) remained largely unaffected. One interpretation is that prion-like spread follows actual neuroanatomical connections available to the introduced seeds; since our injections were in the SNpc (or amygdala in a subset of animals), only regions synaptically linked to those sites developed pathology. Areas like the olfactory bulb or DMV, lacking direct connections to the injection site and potentially having lower local aSyn substrate engagement, were spared.

Our results can be viewed considering studies that have seeded aSyn pathology from peripheral locations. A number of studies have reported limited propagation, whereas others have observed robust propagation from the periphery to the brain. For example, Recasens et al. (2014b) injected an AAV encoding human aSyn into the vagus nerve of rats; they observed aSyn inclusion pathology in vagal-connected brainstem regions, but it failed to reach the SNpc or induce midbrain neurodegeneration. This suggests that aSyn spread from the periphery may

require prolonged time or specific conditions, and certain central regions might be relatively resistant or only vulnerable when the propagation is in a particular direction.

In contrast, other studies have demonstrated substantial pathology moving from peripheral sites toward the brain. Holmqvist et al. (2014) provided direct evidence that aSyn can travel from gut to brain: they showed that aSyn (either from PD brain lysate or recombinant fibrils) injected into the intestinal wall was transported via the vagus nerve and reached the dorsal motor nucleus of the vagus (DMV) in the brainstem within days (Holmqvist et al., 2014). Kim et al. (2019) extended this by injecting PFFs into the mouse gastrointestinal tract and observing a progressive, time-dependent spread of pathology that first appeared in the DMV, then in other connected nuclei such as the locus coeruleus, amygdala, and ultimately the SNpc and even forebrain regions (Kim et al., 2019). Notably, the accumulation of aSyn pathology in Kim's study was accompanied by the loss of dopamine neurons and PD-like motor and cognitive deficits, essentially recapitulating Braak-like staging in an experimental model. However, attempts to initiate aSyn spread from peripheral sites did not yield CNS pathology. Neither intranasal (olfactory) nor gastrointestinal (enteric) PFF injections produced any detectable pS129 aggregates or neurodegeneration in the brain up to 12 months post-injection. This outcome aligns with the previously mentioned Recasens study and underscores the idea of selective network vulnerability in our model. The discrepancy between our negative finding and the robust gut-to-brain propagation seen by Holmqvist, Kim, and others could relate to differences in experimental design. Factors such as the precise injection site and depth (e.g. ensuring fibrils are delivered close to vagal innervation or olfactory neurons), the total fibril load and strain used, the animal species/strain and age (our study used aged rats, which may have slower axonal transport or a shorter remaining lifespan than the young rodents used by Kim et al.), or the duration of the post-injection follow-up could all influence the outcomes. It may be that a longer time or a more permissive environment is required in rats for peripheral seeding to reach the midbrain. In any case, our findings reinforce that aSyn's prion-like spread in vivo is highly dependent on neural connectivity and regional susceptibility: the pathology disseminated chiefly along the pathways emanating from the injection sites (SNpc or amygdala), and it did not naturally jump to distal, unconnected areas like the olfactory bulb or caudal brainstem in the timeframe studied. The fact that we observed widespread aggregate deposition with both SNpc and amygdala injections illustrates that aSyn pathology can be initiated in different brain regions and will propagate along their respective neural networks, rather than strictly adhering to one anatomical starting point. This network-dependent spread

is congruent with the selective pattern of Lewy pathology in PD, where certain circuits are affected while others are spared.

Furthermore, in our study injections into amygdala highlight that the connectivity of the injection site strongly influences aSyn propagation patterns. Injecting PFF into the amygdala primarily led to aSyn aggregate spread within limbic regions such as the hippocampus, without any significant impact on midbrain dopamine neurons in the SNpc. This aligns with recent findings Lai et al., (2025) where amygdala-seeded pathology remained largely within limbic circuits, contrasting with more widespread propagation seen after injections in regions like the dorsal striatum. These observations suggest that some brain regions act as central hubs capable of widely disseminating pathology, while others have more restricted propagation patterns. Additionally, the absence of neurodegeneration in SNpc neurons after amygdala injection indicates differential neuronal vulnerability, with limbic neurons appearing more resistant to immediate aSyn-induced cell death compared to nigral dopamine neurons.

Our model also showed that the injections in amygdala and SNpc and its direct projections were the primary sites for spreading aSyn, while regions with weaker connections, like the DMV or olfactory bulb, were spared, which aligns with the selective pattern of PD pathology. The widespread deposition of aggregates observed with in the groups receiving amygdala and SNpc injections further reinforces the idea that aSyn pathology can initiate in different brain areas and spread through the brain in a manner dependent on network connectivity rather than specific anatomical pathways. This directly addresses our hypothesis that injection site determines spread.

4.2 Nigrostriatal neurodegeneration and neuronal recovery

A key result of this study was the significant loss of TH-positive dopamine neurons in the SNpc after 6 months of PFF seeding in SNpc. However, we observed an unexpected partial restoration of TH signal in the SNpc-injected animals at 12 months post seeding. By 6 months post-injection, roughly half of the SNpc dopamine neurons were lost on the affected side, accompanied by a commensurate reduction in striatal TH-positive fiber density. Such early losses are in line with other toxin and gene-based PD models – for instance (Kirik et al., 2002) reported 30–80% nigral cell loss and ~50% striatal dopamine depletion within 8 weeks after AAV-mediated aSyn overexpression. In our study, this early damage phase likely reflects the

toxicity of aggregated aSyn and associated processes (e.g. microglial activation, axonal pathology) that impair neuronal function and viability. Indeed, (Thakur et al., 2017.) observed that the combination of aSyn overexpression and PFF exposure elicited marked microglial and T-cell activation in the SNpc alongside neuron loss. It is conceivable that in the first months after our AAV-aSyn+ PFF injection, a similar neuroinflammatory and toxic environment led to the rapid degeneration of a subset of vulnerable neurons.

However, a striking finding was that between the 6 and 12 months time points, the extent of dopamine cell loss did not continue to worsen; instead, the remaining TH-positive neurons in SNpc appeared to "rebound" in number or at least in phenotype (with TH immunoreactivity rising to about 80% of the control side from ~50% at the earlier time point). Likewise, striatal dopamine fiber density stabilized rather than declining further. One interpretation is that the neurodegenerative process plateaued after an initial peak of toxicity. Surviving SNpc neurons may have engaged compensatory mechanisms to withstand the chronic presence of aSyn aggregates. Kirik et al., (2002) notably found that by 6 months after initiating aSyn overexpression, the pathological inclusions and axonal dystrophy in surviving nigral neurons had actually subsided compared to the earlier stages, despite continuous high levels of aSyn. They inferred that the neurons which endured the initial insult were able to recover functionally even in the face of sustained aSyn burden. Our results closely parallel this observation as it appears that once a critical threshold of neuron loss was reached by 6 months, the pressure on the system might have eased – either because particularly susceptible neurons had already been eliminated, leaving a more resistant population, or because homeostatic plasticity kicked in to stabilize the system.

Compensatory neuroplasticity in the nigrostriatal pathway is a well-documented phenomenon in PD models and early disease. Surviving dopamine neurons can increase their dopamine output, upregulate enzymes like TH, and even sprout new axonal branches to reinnervate denervated striatal territory. Evidence for such axonal sprouting comes, for example, from partial lesion studies from (Tanguay et al., 2021) showed that when about half of SNpc dopamine neurons were lesioned in neonatal rats, the remaining neurons underwent "massive compensatory sprouting" of their axons. This resulted in a much smaller decrease in striatal dopamine innervation than expected from the cell loss. In our adult model, neuroplastic sprouting may be more limited than in neonates, but even a modest degree of axonal remodeling could explain the stabilization of striatal TH fiber density by 12 months. Additionally, the increase in TH-positive cell count we observed at 12 months could reflect a restoration of

detectable TH expression in neurons that were still alive at 6 months but had downregulated TH due to stress. There is precedent for dopamine neurons transiently losing their phenotype (becoming “TH-negative” despite being alive) under pathological conditions and later re-expressing TH if conditions improve. The reduced presence of active neurotoxic processes at the later time point (for instance, if microglial activation and oxidative stress declined after the initial insult) might have permitted such recovery of function in some neurons.

The partial restoration of TH in our study is promising, suggesting some resilience in the nigrostriatal pathway despite widespread aSyn pathology. However, it raises the question of whether this recovery is a true functional restoration or just a change in phenotype, needing more research on dopamine release or motor behavior to confirm its significance.

In our model, SNpc injections induced significant neurodegeneration and widespread aSyn aggregates in the striatum, whereas amygdala, nasal, or gut injections caused minimal pathology. This selective vulnerability of SNpc dopamine neurons mirrors human PD and aligns with mechanistic studies highlighting their uniquely extensive axonal networks and higher metabolic demands, increasing susceptibility to stress and protein aggregation (Ni & Ernst, 2022; Tanguay et al., 2021).

Although our study offers important insights, it has several limitations that should be noted. First, the limited sample size reduces both statistical power and the ability to generalize the results. The variability in aSyn pathology and neurodegeneration between animals makes it difficult to confidently identify subtle effects. Increasing the cohort size in future experiments would help validate our findings. Second, the study only included two post-injection time points (6 and 12 months), missing earlier stages of disease progression. Additional time points, like 3 and 9 months, would provide a clearer timeline of pathology and recovery, and help capture dynamic processes like axonal sprouting or delayed spread. Thirdly, the animals used were aged while some animals died during the study and since age is a prime factor, using younger animals could have given more robust models as documented in previous studies (Singh et al., 2024). Furthermore our analysis focused on TH immunohistochemistry and pS129 staining, without examining factors like soluble aSyn levels, inflammation markers. Therefore, our interpretation of neuroplastic compensation relies mainly on anatomical data. Future studies with biochemical assays and functional tests would clarify whether recovery is true or compensatory.

4.3 Future prospects

This study provides important implications for understanding PD progression and for developing disease models. The prion-like transmission of aSyn aggregates we observed reinforces the emerging view that PD extends beyond a localized substantia nigra disorder to a progressive protein misfolding disease that propagates throughout the brain over time. Our results align with the idea that interventions in PD might need to target not only the initial triggers of aSyn pathology but also its inter-neuronal transmission. Therapies aimed at blocking aSyn spread (for example, anti-aSyn antibodies or compounds that inhibit cell-to-cell transfer) could potentially slow the progression of pathology through the brain, as suggested by preclinical studies (Tran et al., 2014). The AAV-aSyn + PFF rat model demonstrates a blend of features that resemble mid- to late-stage PD (notably SNpc degeneration and Lewy-like inclusions in multiple brain regions) while also revealing the limits of how far pathology naturally spreads from a given locus. This suggests that a single model may not represent all facets of PD, and different models (or multi-site injection sites as attempted here) might be necessary to simulate the full spectrum of Lewy pathology. Additionally, this model could explore whether blocking aSyn seeding or promoting axonal regeneration protects the SNpc and enhances partial recovery. Nonetheless, the model is a valuable platform for testing therapeutic strategies that aim to halt or reverse neurodegeneration.

5 Conclusion

Our combined overexpression and PFF-seeding rat model replicates the key aspects of PD pathology – notably, the propagation of aSyn aggregates across interconnected brain regions and the selective degeneration of SNpc dopamine neurons – while also revealing the limits and complexities of this propagation. The region-dependent outcomes (severe nigrostriatal damage vs. limited peripheral effects) underscore that PD may involve multiple entry points of pathology but that the substantive neurodegeneration occurs when critically vulnerable populations (like SNpc neurons) are engaged. Our model is an attempt at creating platforms and tools for testing such disease-modifying strategies. By improving understanding of how aSyn aggregates disseminate and cause damage and how the brain reacts over time, we move closer to interventions that could interrupt the progression of PD and perhaps even repair some

of the neural damage it inflicts. Ultimately, these findings deepen our understanding of PD progression and identify potential therapeutic targets to alter its course.

References

Braak, H., Del Tredici, K., Rüb, U., De Vos, R. A. I., Jansen Steur, E. N. H., & Braak, E. (2003). Staging of brain pathology related to sporadic Parkinson's disease. Neurobiology of Aging, 24(2), 197–211. httpre://doi.org/10.1016/S0197-4580(02)00065-9

Calabresi, P., Mechelli, A., Natale, G., Volpicelli-Daley, L., Di Lazzaro, G., & Ghiglieri, V. (2023). Alpha-synuclein in Parkinson's disease and other synucleinopathies: from overt neurodegeneration back to early synaptic dysfunction. Cell Death & Disease 2023 14:3, 14(3), 1–16. https://doi.org/10.1038/s41419-023-05672-9

Chen, M. ;, Mor, D. E., Chen, M., & Mor, D. E. (2023). Gut-to-Brain aSyn Transmission in Parkinson's Disease: Evidence for Prion-like Mechanisms. International Journal of Molecular Sciences 2023, Vol. 24, Page 7205, 24(8), 7205. https://doi.org/10.3390/IJMS24087205

Duffy, M. F., Collier, T. J., Patterson, J. R., Kemp, C. J., Fischer, D. L., Stoll, A. C., & Sortwell, C. E. (2018a). Quality over quantity: Advantages of using alpha-synuclein preformed fibril triggered synucleinopathy to model idiopathic Parkinson's disease. Frontiers in Neuroscience, 12(SEP), 402212. https://doi.org/10.3389/FNINS.2018.00621/BIBTEX

Fujiwara, H., Hasegawa, M., Dohmae, N., Kawashima, A., Masliah, E., Goldberg, M. S., Shen, J., Takio, K., & Iwatsubo, T. (2002). aSyn is phosphorylated in synucleinopathy lesions. Nature Cell Biology, 4(2), 160–164. https://doi.org/10.1038/NCB748,

Hassani, S., & Esmaeili, A. (2024). The neuroprotective effects of ferulic acid in toxin-induced models of Parkinson's disease: A review. Ageing Research Reviews, 97, 102299. https://doi.org/10.1016/j.arr.2024.102299

Holmqvist, S., Chutna, O., Bousset, L., Aldrin-Kirk, P., Li, W., Björklund, T., Wang, Z. Y., Roybon, L., Melki, R., & Li, J. Y. (2014). Direct evidence of Parkinson pathology spread from the gastrointestinal tract to the brain in rats. Acta

Neuropathologica, 128(6), 805–820. https://doi.org/10.1007/S00401-014-1343-6,

Jellinger, K. A. (2011). Synuclein deposition and non-motor symptoms in Parkinson disease. Journal of the Neurological Sciences, 310(1–2), 107–111. https://doi.org/10.1016/J.JNS.2011.04.012

Kim, S., Kwon, S. H., Kam, T. I., Panicker, N., Karuppagounder, S. S., Lee, S., Lee, J. H., Kim, W. R., Kook, M., Foss, C. A., Shen, C., Lee, H., Kulkarni, S., Pasricha, P. J., Lee, G., Pomper, M. G., Dawson, V. L., Dawson, T. M., & Ko, H. S. (2019). Transneuronal Propagation of Pathologic aSyn from the Gut to the Brain Models Parkinson's Disease. Neuron, 103(4), 627-641.e7. https://doi.org/10.1016/J.NEURON.2019.05.035/ATTACHMENT/1A9A8980-1B97-4DB7-9B93-7E5277454C74/MMC7.PDF

Kirik, D., Rosenblad, C., Burer, C., Lundberg, C., Johansen, T., Muzyczka, N., Mandel, R., & Björklund, A. (2002). Parkinson-like neurodegeneration induced by targeted overexpression of alpha-synuclein in the nigrostriatal system. The Journal of Neuroscience, 22(7), 2780–2791. https://portal.research.lu.se/en/publications/parkinson-like-neurodegeneration-induced-by-targeted-overexpressi

Lai, T. T., Xiang, W., Stanojlovic, M., Käufer, C., Feja, M., Lau, K., Zunke, F., & Richter, F. (2025). The basolateral amygdala and striatum propagate alpha-synuclein pathology causing increased fear response in a Parkinson's disease model. Brain, Behavior, and Immunity, 128, 469–486. https://doi.org/10.1016/J.BBI.2025.04.025

Li, J. Y., Englund, E., Holton, J. L., Soulet, D., Hagell, P., Lees, A. J., Lashley, T., Quinn, N. P., Rehncrona, S., Björklund, A., Widner, H., Revesz, T., Lindvall, O., & Brundin, P. (2008). Lewy bodies in grafted neurons in subjects with Parkinson's disease suggest host-to-graft disease propagation. Nature Medicine, 14(5), 501–503. https://doi.org/10.1038/NM1746,

Luk, K. C., Kehm, V., Carroll, J., Zhang, B., O'Brien, P., Trojanowski, J. Q., & Lee, V. M. Y. (2012a). Pathological aSyn Transmission Initiates Parkinson-like Neurodegeneration in Non-transgenic Mice. Science (New York, N.Y.), 338(6109), 949. https://doi.org/10.1126/SCIENCE.1227157

Ni, A., & Ernst, C. (2022). Evidence That Substantia Nigra Pars Compacta Dopamine Neurons Are Selectively Vulnerable to Oxidative Stress Because

They Are Highly Metabolically Active. Frontiers in Cellular Neuroscience, 16, 826193. https://doi.org/10.3389/FNCEL.2022.826193

Poewe, W., Seppi, K., Tanner, C. M., Halliday, G. M., Brundin, P., Volkmann, J., Schrag, A. E., & Lang, A. E. (2017). Parkinson disease. Nature Reviews Disease Primers, 3, 1–21. https://doi.org/10.1038/NRDP.2017.13,

Recasens, A., Dehay, B., Blesa, J., & Herva, M. E. (2014). Alpha-synuclein spreading in Parkinson's disease. Frontiers in Neuroanatomy, 8(DEC), 159. https://doi.org/10.3389/FNANA.2014.00159

Schintu, N., Frau, L., Ibba, M., Garau, A., Carboni, E., & Carta, A. R. (2009). Progressive dopamine degeneration in the chronic MPTPp mouse model of parkinson's disease. Neurotoxicity Research, 16(2), 127–139. https://doi.org/10.1007/S12640-009-9061-X,

Singh, A., Panhelainen, A., Reunanen, S., Luk, K. C., & Voutilainen, M. H. (2024). Combining fibril-induced alpha-synuclein aggregation and 6-hydroxydopamine in a mouse model of Parkinson's disease and the effect of cerebral dopamine neurotrophic factor on the induced neurodegeneration. European Journal of Neuroscience, 59(1), 132–153. https://doi.org/10.1111/EJN.16196,

Spillantini, M. G., Schmidt, M. L., Lee, V. M. Y., Trojanowski, J. Q., Jakes, R., & Goedert, M. (1997). aSyn in Lewy bodies [8]. Nature, 388(6645), 839–840. https://doi.org/10.1038/42166;KWRD=SCIENCE

Tanguay, W., Ducrot, C., Giguère, N., Bourque, M. J., & Trudeau, L. E. (2021). Neonatal 6-OHDA lesion of the SNc induces striatal compensatory sprouting from surviving SNc dopamine neurons without VTA contribution. The European Journal of Neuroscience, 54(7), 6618–6632. https://doi.org/10.1111/EJN.15437

Thakur, P., Breger, L. S., Lundblad, M., Wan, O. W., Mattsson, B., Luk, K. C., Lee, V. M. Y., Trojanowski, J. Q., & Björklund, A. (n.d.). Modeling Parkinson's disease pathology by combination of fibril seeds and aSyn overexpression in the rat brain. https://doi.org/10.1073/pnas.1710442114

Tran, H. T., Chung, C. H. Y., Iba, M., Zhang, B., Trojanowski, J. Q., Luk, K. C., & Lee, V. M. Y. (2014). aSyn Immunotherapy Blocks Uptake and Templated Propagation of Misfolded aSyn and Neurodegeneration. Cell Reports, 7(6), 2054–2065. https://doi.org/10.1016/J.CELREP.2014.05.033

Visanji, N. P., Brooks, P. L., Hazrati, L. N., & Lang, A. E. (2014). The prion hypothesis in Parkinson's disease: Braak to the future. Acta Neuropathologica

Communications, 2(1), 1–12. https://doi.org/10.1186/2051-5960-1-2/FIGURES/1

Volpicelli-Daley, L. A., Luk, K. C., & Lee, V. M. Y. (2014). Addition of exogenous aSyn preformed fibrils to primary neuronal cultures to seed recruitment of endogenous aSyn to Lewy body and Lewy neurite–like aggregates. Nature Protocols 2014 9:9, 9(9), 2135–2146. https://doi.org/10.1038/nprot.2014.143